Silicon (2018) 10:1151–1159
https://doi.org/10.1007/s12633-017-9587-0

ORIGINAL PAPER

FTIR Spectral Characterization, Mechanical Properties and Antimicrobial Properties of La-Doped Phosphate-Based Bioactive Glasses

Rasha A. Youness[1] · Mohammed A. Taha[2] · Medhat Ibrahim[1] · Amany El-Kheshen[3]

Received: 28 November 2016 / Accepted: 26 May 2017 / Published online: 3 October 2017

Abstract $(Na_2O)_{0.20}(CaO)_{0.14}(P_2O_5)_{0.66-x}(La_2O_3)_x$, where x=0, 0.1, 0.3, 0.7 and 1 wt.%, was prepared by the conventional melt-quenching method. Physical and mechanical properties such as density, Vickers microhardness, compressive strength and fracture toughness were measured for all prepared glass samples. In order to evaluate in-vitro bioactivity of the prepared glasses, sample powders (particle size range 106-180 μm) were soaked in simulated body fluid (SBF) solution at 37 ± 0.5 °C for 7, 14 and 21 days. Then, soaked samples were investigated by Fourier transform infrared (FTIR) spectroscopy, X-ray diffraction (XRD) technique and transmission electron microscopy (TEM). Furthermore, the antimicrobial activity of these glasses was tested against *E. coli*, *S. aureus*, *B. cereus, B. subtilis and C. albicans* by the disc-diffusion method. The obtained results indicated that significant increases in density, mechanical properties and antibacterial activity against *S. aureus* and *E. coli* bacteria were obtained as the La content increases. XRD and FTIR spectra revealed that the bioactivity of the prepared glasses was not affected by increasing of the La content. These results suggested that these glasses can be extensively used in various biomedical applications.

Keywords FTIR characterization · Mechanical properties · Antimicrobial activity · In-vitro bioactivity

1 Introduction

There is a growing need for soft and/or hard tissue replacements for enhanced tissue regeneration. Therefore, biodegradable materials possessing controllable and particular bioactivity are required [1]. In order to achieve these demands, various inorganic bioactive materials including calcium phosphate ceramics, hydroxyapatite (HA) and bioactive glasses (BGs) are used in clinics and give excellent results [2].

BGs can be utilized extensively as bone substitutes. When these glasses are exposed to phosphate solutions such as simulated body fluid (SBF), they form a HA, or hydroxycarbonated apatite (HCA), layer on their surfaces within a few days and this layer is responsible for the formation of chemical bond between the glasses and host bone tissue giving an indication for their behavior in-vivo [3–5]. Moreover, many studies report that the leached ions that are released from bioglasses are able to induce cell proliferation as well as differentiation of osteoblasts [6]. According to these unique properties, bioglasses have received great attention for use in many biomedical fields.

There are many published articles concentrated on silica-based glasses. Unfortunately, the long-term effect of silicon on the human body has not been studied well. In order to avoid this uncertain effect of silicon on human health, phosphate-based glasses are desirable for orthopaedic

✉ Rasha A. Youness
rhakamnrc@gmail.com

[1] Spectroscopy Department, National Research Centre, El Buhouth St., Dokki, Cairo 12622, Egypt

[2] Solid-State Physics Department, National Research Centre, El Buhouth St., Dokki, Cairo, 12622, Egypt

[3] Glass Research Department, National Research Centre, El Buhouth St., Dokki, Cairo, 12622, Egypt

implants due to their biocompatibility and biodegradability in water, SBF solution and body fluids [7–9]. This degradation can be controlled to change significantly and suit many tissue engineering applications [10]. Despite these great advantages, biomedical applications of phosphate-based glasses are limited due to their poor mechanical properties and low chemical durability [1].

The influence of rare earth (RE) elements on the human body acquires great interest in orthopaedic fields. RE includes all lanthanides such as Lanthanum (La), Cerium (Ce) and Praseodymium (Pr) those can replace calcium (Ca^{2+}) ions in apatite and therefore, they are called Ca-substituting ions in apatite [11]. The effect of addition of La to bioceramics has been studied by several authors. Serret et al. [12] showed that the addition of La to HA causes more stabilization in its structure. Shin-Ike et al. [13] observed significant increase in mechanical properties of La-substituted HA compared to La-free HA. Fernandez et al. [14] found that the substitution of La for Ca in HA is responsible for better resistance of bone to acid degradation. Zhang et al. [15] reported that La inhibits the resorption of bones. Moreover, when it is added to bioglasses, it enhances their mechanical properties [11, 16]. This means that the La-containing bioceramics are promising in dental and orthopaedic implants.

Based upon the above considerations, the influence of incorporation of lanthanum in phosphate-based glasses on the bioactivity, density, mechanical and antimicrobial properties was investigated.

2 Experimental Work

2.1 Glass Preparation

Melt quenched $(Na_2O)_{0.14}(CaO)_{0.24}(P_2O_5)_{0.66-x}(La_2O_3)_x$, where x = 0, 0.1, 0.3, 0.7 and 1 wt.%, glasses have been prepared from starting materials of analytical reagent grade. Sodium carbonate (Na_2CO_3), calcium carbonate ($CaCO_3$), ammonium dihydrogen phosphate ($NH_4H_2PO_4$) and La_2O_3 powders were mixed very well in the appropriate quantities and then ground in an agate mortar. The weighed well-mixed batches were melted in a porcelain crucible in an electric furnace at 1200-1250 °C for 2 h in air. The molten liquid was occasionally stirred to ensure homogeneous mixing of all constituents and to obtain bubble-free samples. The glass, formed by quenching the melt on a stainless-steel mold, was immediately transferred to another muffle furnace where it was annealed at about 350 °C for 1 h. Then, the muffle was switched off and the temperature decreased to room temperature with a rate of 25 °C/h. The nominal compositions of the prepared glasses together with their abbreviations are given in Table 1.

Table 1 Nominal composition (wt.%) of La-containing phosphate glasses

Glass name	Chemical composition (wt.%)			
	Na_2O	CaO	P_2O_5	La_2O_3
La0	20	14	66	0
La0.1	20	14	65.9	0.1
La0.3	20	14	65.7	0.3
La0.7	20	14	65.3	0.7
La1	20	14	65	1

2.2 Measurements of Physical Properties

2.2.1 Density and Mechanical Properties

The density (ρ) of each glass sample was measured at room temperature using Archimedes method with water as the immersion liquid.

Vickers microhardness (H_V) of the 2 mm thick polished samples was measured with a Shimadzu-HMV (Japan) microhardness tester using 100 g load under ambient laboratory conditions with a constant indenter dwell time of 15 s. At least five indentations were measured per specimen for each data point. The indentation was made using a square based pyramidal diamond with face angle 136°and measuring microscope as well as a video monitor. Vickers microhardness was calculated using Eq. 1 and according to ASTM: B933-09, by finding the ratio of the applied load to the pyramidal contact area of the indentation [17]:

$$H_V = 1.854P/D^2 \quad (1)$$

where P is the applied indentation load and D is the measured indentation diagonal. The fracture toughness, K_{IC}, of the samples was determined from the indentation fracture using the Vickers microhardness tester. K_{IC} was calculated using the following equation [18, 19]:

$$K_{IC} = 0.016H_V\frac{a^2}{c^{3/2}} \quad (2)$$

where a is the diagonal half length of the indent and c is the crack length from the center of the indentation to the crack end. On the other hand, compressive strength was calculated according to ASTM E9.

2.3 In Vitro Bioactivity Evaluation

According to ISO 23317 approved in June 2007 by the International Organization for Standardization, the SBF solution is frequently used to evaluate in-vitro bioactivity of the prepared glasses by soaking samples in this solution for different time intervals. The SBF is prepared according to the

recipe described by Kokubo et al. [20, 21] and its ionic concentration is closely similar to that found in human plasma as presented in Table 2. In order to use an excess SBF volume surrounding the glass grains, the ratio of 0.01 g/ml suggested by Siqueira and Zanotto [22] is utilized in this work. Therefore, the glasses were ground in an agate mortar, sieved to obtain fine particles in the size range of 106-180 μm and used for antimicrobial and bioactivity measurements. About 500 mg of the glass powders, with such particle sizes, was washed ultrasonically in acetone for a few minutes, left to air-dry and then placed in polyethylene bottles containing 50 mL of SBF at 37 ± 0.5 °C for different time intervals, i.e. 7, 14 and 21 days. After soaking in the SBF for the specified test time, the samples were taken out of the bottles and dried at room temperature. The formation of the HA-like layer on the surfaces of soaked glass powders was followed up by FTIR spectroscopy and the XRD technique.

2.4 Characterization of Glasses after Soaking

FTIR spectra of the glasses, before and after soaking, were obtained at room temperature using the KBr pellet method by an infrared spectrophotometer type (Vertex 70) in the wavenumber range of 2000-400 cm^{-1} using 100 scans at 2 cm^{-1} resolution.

A pH meter (Jenway 3510) was employed also to monitor the changes that occurred during the immersion of glass grains of the investigated samples in SBF solution. Three measurements, at each time, were carried out and the mean value is calculated to ensure the reproducibility of the readings.

To demonstrate the antimicrobial effect of the prepared glass samples, some microorganisms such as *S. aureus*, *B. cereus, B. subtilis as* Gram+, *E. coli* as Gram– bacteria and *C. albicans* are used.

3 Results and Discussion

3.1 Density Measurements

Figure 1 shows the density of all investigated glasses as a function of La_2O_3 content. The figure indicates a considerable increase in densities of the prepared glasses as the La_2O_3 content increases. The substitution of a lighter element such as P_2O_5 (density=2.39 g/cm^3) with a heavier one such as La_2O_3 (density=6.51 g/cm^3) is the main reason for such an increase in density values of the prepared glasses. Similar results were reported in Refs. [23, 24].

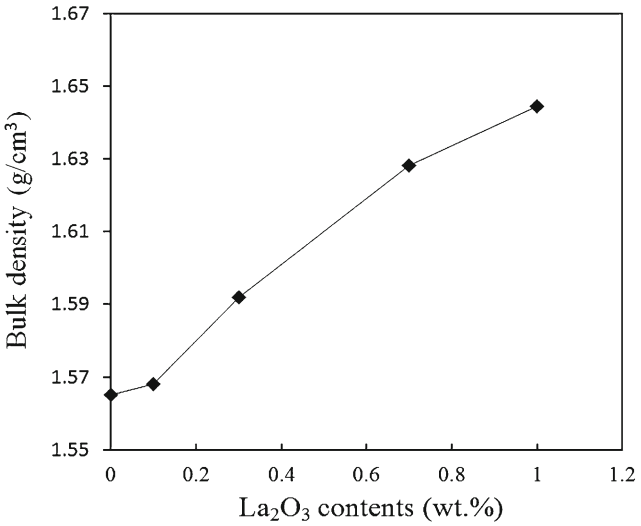

Fig. 1 The effect of La_2O_3 contents (wt.%) on the bulk density of prepared glasses

3.2 Mechanical Properties

It is well known that the fracture toughness of bioglasses is lower than that of bone. Therefore, the enhancement of their toughness is essential [25]. In order to achieve this purpose, La_2O_3 was added to phosphate-based glasses. Vickers microhardness, fracture toughness and compressive strength of all glass specimens were measured and represented in Figs. 2 and 3, respectively. From these figures, significant increases in hardness and compressive strength are observed, while a slight increase in fracture toughness is recorded as La_2O_3 content increases. These results are strongly correlated to the obtained density measurements discussed in the previous section, i.e. the increase of glass density contributes to the enhancement of compactness of the glass structure and as a consequence, better microhardness values are obtained [26]. These results are similar to

Table 2 Ionic concentration (mM) of simulated body fluid (SBF) and human blood plasma

Solution	Ion concentration (mM)							
	Na^+	K^+	Mg^{2+}	Ca^{2+}	$C1^-$	HCO_3^-	HPO_4^{2-}	SO_4^{2-}
SBF	142.0	5.0	1.5	2.5	147.8	4.2	1.0	0.5
Blood plasma	142.0	5.0	1.5	2.5	103.0	27.0	1.0	0.5

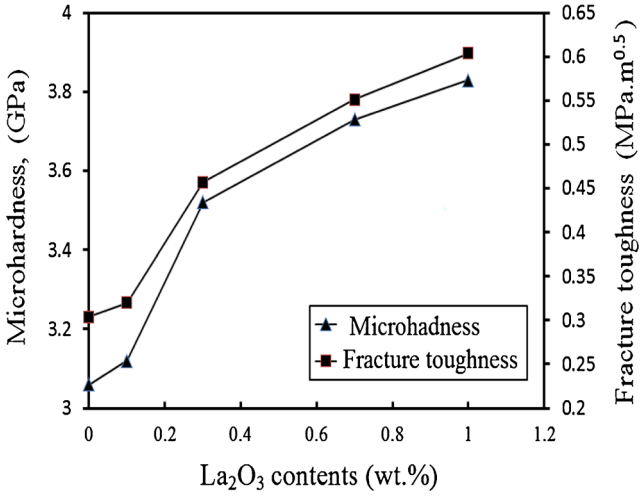

Fig. 2 The measured microhardness and fracture toughness as a function of La content (wt.%)

those reported in Ref. [27]. According to their appropriate mechanical properties, these glasses are recommended in load-bearing sites applications such as orthopaedic as well as dental applications [28] (Figs. 2 and 3).

3.3 XRD Analysis

The formation of a HA-like layer on the glass surface is essential for forming a firm bond with human bone when inserted into the body [29]. The formation of the HA layer on the surface of glass grains is occurred as a result of their dissolution, precipitation and ion exchange. When bioglass is soaked in SBF solution, a partial degradation of the surface starts instantly, therefore, Ca^{2+}, HPO_4^{2-} and PO_4^{3-} ions

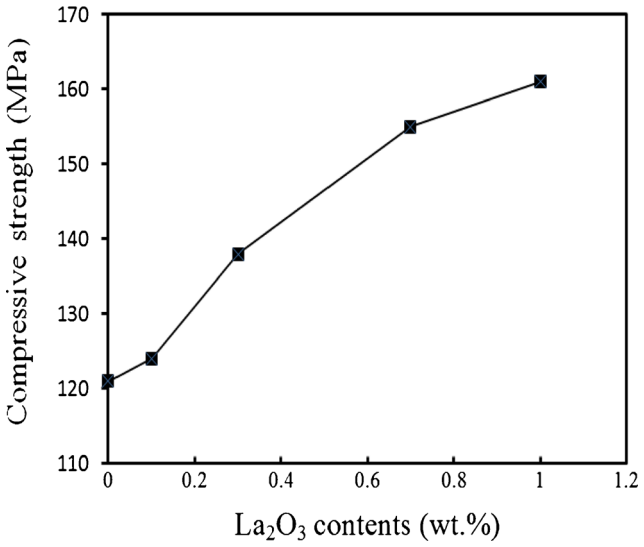

Fig. 3 Compressive strength of investigated samples versus La content (wt.%)

are liberated and as a consequence, a HA layer is formed [30]. Accordingly, the formation of such a layer on the surfaces of all studied glass specimens after soaking in SBF solution for 7, 14 and 21 days, along with the as-prepared glasses, was followed up by the XRD technique and shown in Fig. 4a–d.

As seen in Fig. 4a, the amorphous nature of the prepared glasses is confirmed by the absence of sharp peaks. Based on XRD card no. 72-1243, the presence of the most intense peaks at $2\theta = 31.8$, 32.9, 32.2, 25.9, 46.66 and 49.46°, corresponding to (2 1 1), (3 0 0), (1 1 2), (0 0 2), (2 2 2), (2 1 3) reflections, respectively, refers to the formation of HA-like layer on the surface of the glass samples. As indicated from Fig. 4b, the peak at $2\theta = 31.8°$ is distinctly observed after 7 days of soaking for all glass samples. After 14 days of glass soaking in solution, as shown in Fig. 4c, overlapped peaks at $2\theta = 32.9$ and 32.2° are obviously detected and the peak at $2\theta = 31.8°$ becomes more developed. New peaks at $2\theta = 25.9$, 49.46, 46.66° appear after 21 days of immersion as exhibited in Fig. 4d.

As indicated from the figure, XRD peaks become more intense as soaking time increased suggesting that the HA-like layer grow significantly [6]. This growth is highly influenced by soaking time as the increase of time permits both Ca^{2+} and PO_4^{3-} ions to accumulate on the glass surface resulting in development of the HA layer [31]. Note that these peaks are broad indicating to that the formed apatite is poorly crystallized and/or falls in the nanoscale range [32, 33].

3.4 FTIR Spectral Analysis

In order to investigate the glasses structure, follow up their degradation and the formation of the HA layer on their surfaces after soaking in SBF solution for 7, 14 and 21 days, FTIR spectroscopy was employed and the resultant spectra are shown in Fig. 5a–d. The characteristic FTIR absorption peaks are assigned according to the literature [10, 24, 32, 34–36].

The intense peak at 1253 cm^{-1} with ill-defined one at 1153 cm^{-1} are attributed to asymmetric and symmetric stretching of the two non-bridging oxygen atoms bonded to phosphorous atoms in the Q^2 tetrahedral sites and the symmetric stretching mode of the same structural unit, respectively. However, the intense peak near 1096 cm^{-1} is assigned to symmetric vibrations of the PO_3 group and/or the O-P-O bond. The weak band at 1043 cm^{-1} is attributed to the symmetric stretching mode of the PO_4^{3-} groups. The two shoulders at 778 and 720 cm^{-1} are ascribed to the symmetric vibration of the P-O-P linkage. On the other hand, the peak at 534 cm^{-1} is attributed to the bending vibration of such a linkage. Since the band of ν_{as} (P-O-P) appears at 938 cm^{-1}, these glasses have a chain structure and possess a significant increase of covalency proportion of the P-O-P bond

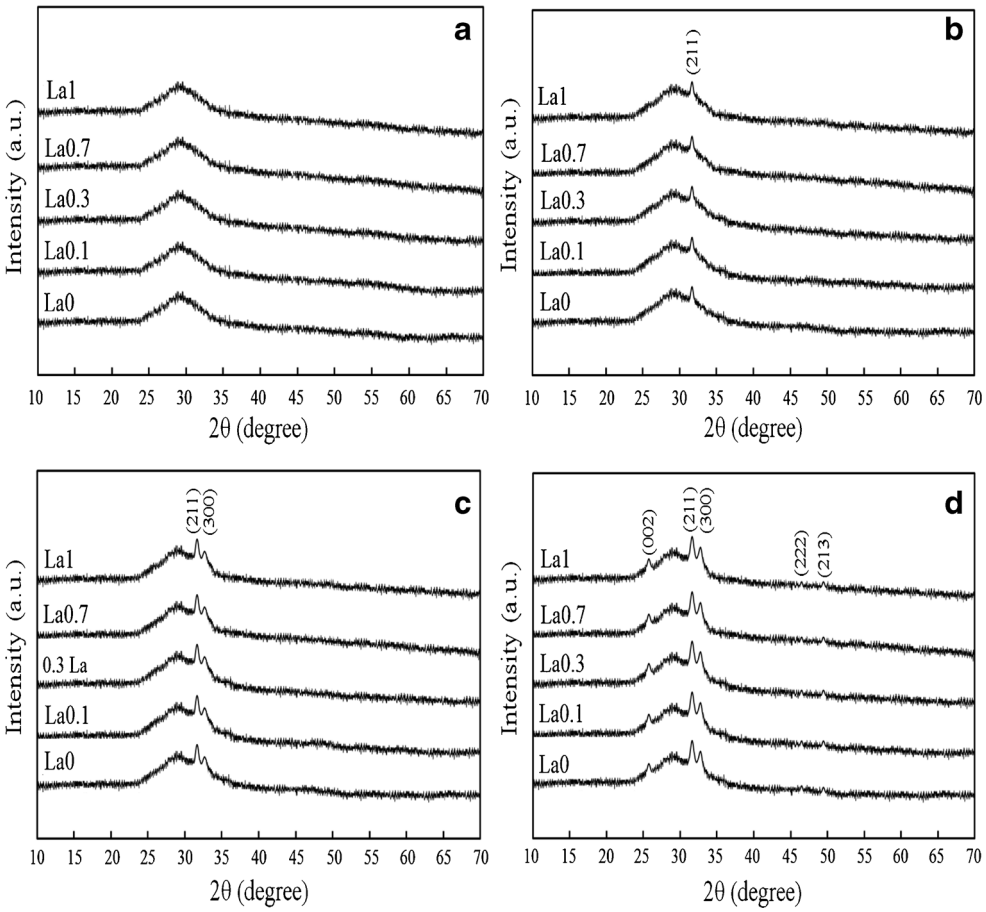

Fig. 4 XRD patterns of **a** as-parent glasses, glasses after immersion in SBF solution for **b** 7 days, **c** 14 days and **d** 21 days

which results in considerable strength and chemical durability. These results are in agreement with those reported in Refs. [35, 36]. The P-O resonance in the PO_4^{3-} group is indicated by two bands at 560 and 605 cm^{-1} which confirm the formation of crystalline HA. The presence of a weak band at 870 cm^{-1} is attributed to P-O-H resonance in HPO_4^{2-}. The two peaks at 1550 and 1640 cm^{-1} are assigned to the C-O resonance in CO_3^{2-}. The dissolution of atmospheric CO_2 into the SBF is responsible for the substitution of CO_3^{2-} ions into the HA lattice. Since the solution contains CO_3^{2-} ions, they are likely to substitute OH^- ions in the HA lattice [37, 38]. The formation of a HCA layer on the glass surface agrees with the results reported by Kokubo et al. [21] who postulated that the immersion of glass grains in SBF produces a HCA layer. Moreover, the bending vibration of the O-H bond of the absorbed water, from air, is found at 1634 cm^{-1} [10]. As anticipated, after 21 days of soaking, HA deposition is increased significantly as indicated by more sharpness and intensification of the two characteristic peaks of HA indicating that the formed HA possesses a reasonable crystallinity degree.

Generally, the existence of network modifiers such as Ca^{2+} and Na^+ in the glass system forms non-bridging oxygens (NBOs) and consequently promotes the dissolution of glass samples in SBF solution. These changes in surface chemistry contribute to the precipitation of a calcium phosphate layer on the sample surface and subsequent crystallization to form crystalline HA [39]. Considering the bioactive behavior of the prepared glass samples after soaking in SBF solution, Na^+ ions are released into the physiological solution through the interchange with the H^+ ions from solution and consequently P-OH groups are formed on the glass surfaces. These groups are able to combine with Ca^{2+} ions, from the SBF solution, to form an amorphous layer of calcium phosphate and turn into bone-like apatite crystals. The following equation clarifies the HA formation [40, 41]:

$$10Ca^{2+} + 6PO_4^{3-} + 2OH^- \rightarrow Ca_{10}(PO_4)_6(OH)_2$$

The raising of supersaturation above the critical level that is required for heterogeneous nucleation of apatite is responsible for the initiation of apatite nuclei. It is worth mention that the degree of supersaturation of SBF, with respect to HA, is further promoted by the increase of liberated Na^+ ions. Once the apatite nuclei are formed, they grow by consuming the Ca^{2+}, PO_4^{3-} and OH^- ions from the solution [42].

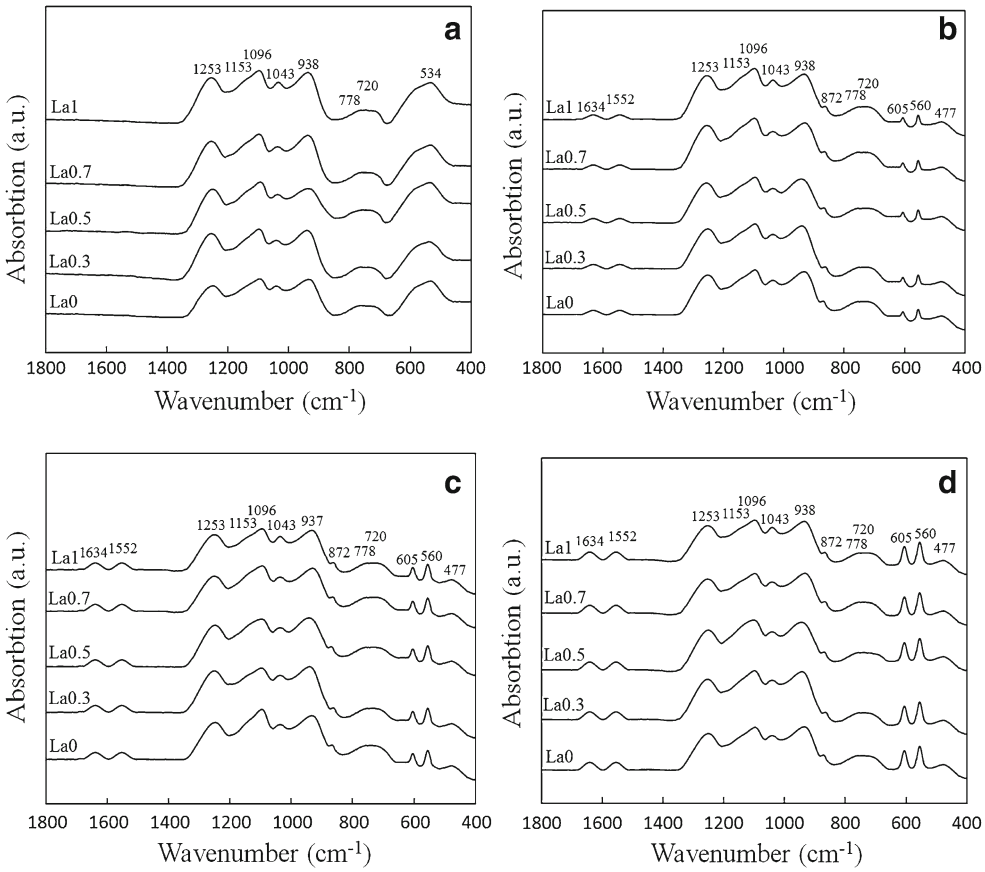

Fig. 5 FTIR spectra of **a** as-parent glasses, glasses after immersion in SBF solution for **b** 7 days, **c** 14 days and **d** 21 days

From the above results, we can conclude that La-containing phosphate glasses are characterized by good bioactivity. Similar results were reported for lanthanide-containing biomaterials and mentioned that lanthanides did not retard the formation of HA on the glass surfaces [6].

3.5 The pH Measurements

Table 3 illustrates the changes of pH values of SBF at the end of soaking time. As indicated from the table, there is a rapid increase in pH values, for all investigated samples, after 7 days of soaking followed by a marked decrease after 14 and 21 days of soaking in SBF solution. The replacement of protons, found in solution, with cationic glass components results in such increase of pH values and consequently the solution becomes alkaline. On the other hand, as the HA-like layer begins the precipitation on the glass surface, this increase is stopped and even decreases slightly. Surprisingly, La^{3+} ions have no considerable effect on pH values due to the fact that they possess ionic radii similar to that of Ca^{2+} ions and consequently charge balance can be easily preserved with a pair of substitutions such as $2Ca^{2+} = La^{3+} + Na^{+}$ [34]. Similar results were reported in Refs. [1, 8, 43, 44]. These measurements are necessary to identify the biocompatibility of these glasses when inserted into the human body [45].

Table 3 The pH measurements of SBF solution after soaking of glass grains for different time intervals

Time (weeks)	La0	La0.1	La0.3	La0.7	La1
0	7.2	7.2	7.2	7.2	7.2
1	8.68	8.68	8.69	8.67	8.69
2	8.44	8.46	8.47	8.47	8.48
3	8.25	8.26	8.26	8.27	8.25

3.6 TEM Observation

TEM was employed to determine the particle size of the formed HCA layer on the surface of La0 and La1 glass samples after soaking in SBF solution for 21 days as shown in Fig. 5a,b. As seen from this figure, the glass grains are nearly covered with hexagonal HA crystallites and they seem to be agglomerate-free. The mean values of the particle sizes of HA are 49 and 43 nm for La0

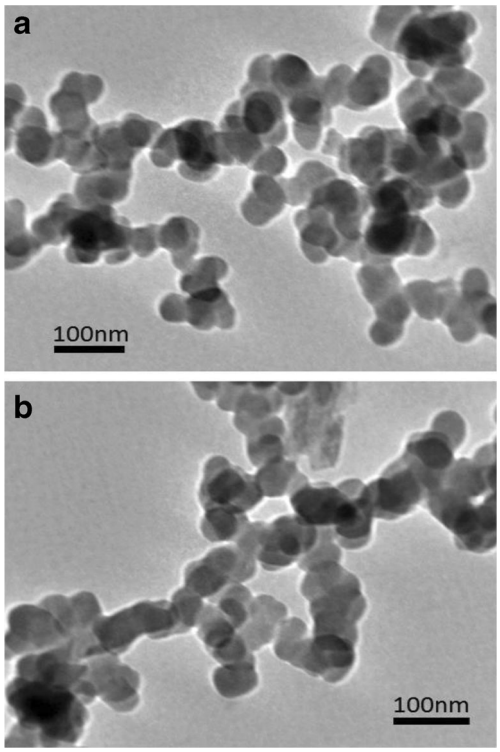

Fig. 6 TEM micrographs of **a** La0 and **b** La1 glass samples after soaking in SBF solution for 21 days

and La1 glass specimens, respectively. These results are in agreement with those obtained from XRD (Fig. 6).

3.7 Antimicrobial Effect

The BG-related infections are considered as the main drawback for using them in medicine as they lead to patient morbidity and as a consequence, acute as well as chronic infections will occur as a result of bacterial colonization and the formation of biofilm [46].

The antimicrobial behavior (Fig. 7) of La_2O_3-free and La_2O_3-containing phosphate glasses were evaluated against *S. aureus* (ATCC6538), *B. subtilis* (NRRL-B-4219), *B. cereus* (local isolate) and *E. coli* (ATCC25922) as Gram+, Gram– bacteria and fungi such as *C. albicans* (ATCC10231) using agar disc-diffusion assays conducted for 24 h at 37 °C. The obtained photographs show that the growth of *S. aureus* is retarded remarkably as La content increases. On the other hand, La has a less powerful effect on *E. coli* than *S. aureus* as the antibacterial behavior is indicated only when the La content is 1 wt.%. Furthermore, La-free glass exhibits a considerable antibacterial effect against these bacteria as a result of pH change, i.e. due to the dissolution of glass and/or minimized activity of water, namely, due to the leaching of ions. It is worth to note that these glasses have no

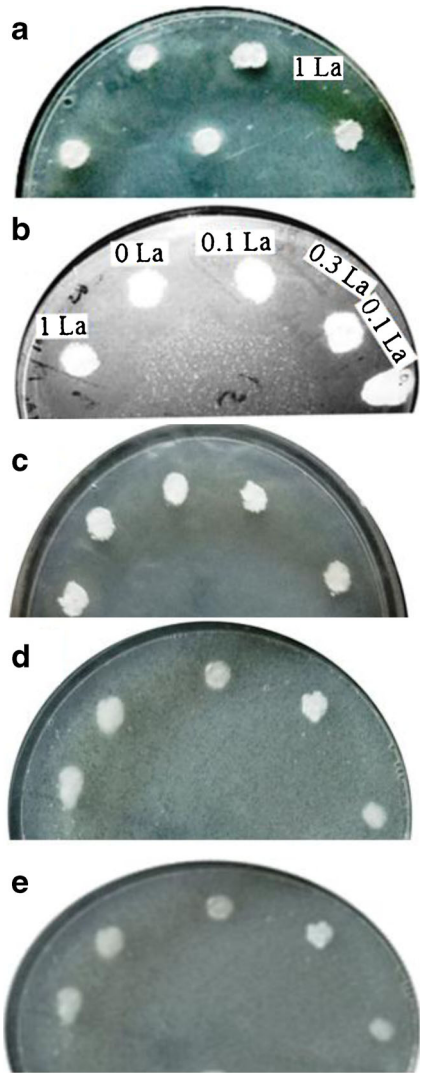

Fig. 7 Petri dish photographs after conducting agar disc-diffusion assays at 37 °C for 24 h against **a** *E. coli*, **b** *S. aureus*, **c** *B. subtilis*, **d** *B. cereus* and **e** *C. albicans* as test micro-organisms for tested glasses

considerable effect against *B. subtilis*, *B. cereus* and *C. albicans*. The diameter of the inhibition zone for all samples is measured and listed in Table 4. The antibacterial behavior of these glasses can be interpreted in terms of the liberation of Ca^{2+}, Na^{+} and PO_4^{3-} ions with high concentrations which contribute to intense disorder of bacterial membrane potential and consequently, acute variations in osmotic pressure take place and lead to destruction in the bacterial cell wall. Subsequently, the degradation as well as the composition of as-prepared glasses in SBF identifies their antibacterial effects [10]. Taking into account that the employed powder systems have elevated surface area this is considered as the main reason for rapid dissolution and therefore, the high rise in local pH [15].

Table 4 The measured inhibition zone diameters of all La-containing phosphate glasses against *S. aureus, B. cereus, B. subtilis, E. coli and C. albicans*

Glass code	Inhibition zone diameter (mm)				
	S. aureus	B. Cereus	B. subtilis	E. coli	C. albicans
La0	25	Nil	Nil	Nil	Nil
La0.1	27	Nil	Nil	Nil	Nil
La0.3	30	Nil	Nil	Nil	Nil
La0.7	32	Nil	Nil	Nil	Nil
La1	38	Nil	Nil	25	Nil

The antimicrobial activity of the parent glass arises from the capability to release Ca^{2+} ions at the glass-particle interface, which leads to membrane depolarization and the subsequent death of the cell. It is well known that cellular calcium ions overload, or perturbation of intracellular Ca^{2+} compartmentalization, may cause cytotoxicity and result in either apoptotic, necrotic or autophagic cell death [46]. Similar results were reported for lanthanide doped glasses [35, 36, 47–50].

4 Conclusions

In the present work, $CaO\text{-}Na_2O\text{-}P_2O_5$ glass system was used to transport La^{3+} ions in a controlled manner. This system has tremendous advantages such as controlled dissolution rates, biocompatibility and bioresorbability. Furthermore, doping of phosphate-based glasses with La^{3+} had an excellent antibacterial effect against *S. aureus* and *E. coli*. On the other hand, other tested microorganisms such as *B. subtilis*, *B. cereus* and *C. albicans* were resistant to this glass system. Moreover, the addition of La^{3+} with successive contents to phosphate-based glasses contributed to considerable enhancement of their mechanical properties without any retardation of their bioactivity. The obtained results suggest that these glasses have promising uses in tissue engineering fields.

References

1. Abou Neel EA, Pickup DM, Valappil SP, Newport RJ, Knowles JC (2009) Bioactive functional materials: a perspective on phosphate-based glasses. J Mater Chem 19:690–701
2. Liu C, Chen C, Ducheyne P (2008) In vitro surface reaction layer formation and dissolution of calcium phosphate cement–bioactive glass composites. Biomed Mater 3:1–22
3. Mohini GJ, Krishnamacharyulu N, Baskaran GS, Veeraiah N (2015) Role of Ga_2O_3 ions on the structural and bioactive behavior of $B_2O_3\text{-}SiO_2\text{-}P_2O_5\text{-}Na_2O\text{-}CaO$ glass systems. Int J Eng Tech Res 3(4):441–447
4. Chen X, Chen X, Brauer DS, Wilson RM, Hill RG, Karpukhina N (2014) Bioactivity of sodium free fluoride containing glasses and glass-ceramics. Mater 7:5470–5487
5. Ravarian R, Moztarzadeh F, Hashjin MS, Rabiee SM, Khoshakhlagh P, Tahriri M (2010) Synthesis, characterization and bioactivity investigation of bioglass/hydroxyapatite composite. Ceram Int 36:291–297
6. Miao G, Chen X, Mao C, Li X, Li Y, Lin C (2014) Synthesis and characterization of europium-containing luminescent bioactive glasses and evaluation of in vitro bioactivity and cytotoxicity. J. Sol-Gel Sci Technol 69:250–259
7. Thonglem S, Rujijanagul G, Eitssayeam S, Tunkasiri T, Pengpat K (2013) Fabrication of $P_2O_5\text{-}CaO\text{-}Na_2O$ glasses doped with maganesium oxide for artificial bone applications. Ceram Int 39:S537–540
8. Majhi MR, Pyare R, Singh SP (2011) Studies on preparation and characterization of $Na_2O\text{-}CaO\text{-}P_2O_5\text{-}ZrO_2$ bioglasses-ceramics. Int J Sci Eng Res 2(8):1–13
9. ElBatal HA, Khalil EMA, Hamdy YM (2009) In vitro behavior of bioactive phosphate glass-ceramics from the system $P_2O_5\text{-}Na_2O\text{-}CaO$ containing titania. Ceram Int 35:1195–1204
10. Ahmed AA, Ali AA, Mahmoud DAR, El-Fiqi AM (2011) Study on the preparation and properties of silver-doped phosphate antibacterial glasses. Sol State Sci 13:981–992
11. Lou W, Dong Y, Zhang H, Jin Y, Hu X, Ma X, Liu J, Wu G (2015) Preparation and characterization of lanthanum-incorporated hydroxyapatite coatings on titanium substrates. Int J Mol Sci 16(9):21070–21086
12. Serret A, Cabanas MV, Vallet-Regi RM (2000) Stabilization of calcium oxyapatites with lanthanum (III)-created anionic vacancies. Chem Mater 12:3836–3841
13. Shin-Ike SM, Tsutsui J, Tanaka A, Murayama S, Fujita A (1989) Attempts to improve the strength of sintered lanthanum-containing hydroxyapatites. Shika Igaku J Osaka Odontol Soc 52:854–861
14. Fernandez-Gavarron F, Huque T, Rabinowitz JL, Brand JG (1988) Incorporation of 140-lanthanum into bones, teeth and hydroxyapatite. Bone Miner 3:283–291
15. Zhang JC, Xu SJ, Wang K, Yu SF (2003) Effects of the rare earth ions on bone resorbing function of rabbit mature osteoclasts in vitro. Chin Sci Bull 48:2170–2175
16. Meenambal R, Singh RK, Kumar PN, Kannan S (2014) Synthesis, structure, thermal stability, mechanical and antibacterial behavior of lanthanum (La^3+) substitutions in β-tricalciumphosphate. Mater Sci Eng C 43:598–606
17. Youness RA, Taha MA, Elhaes H, Ibrahim M (2017) Molecular modeling, FTIR spectral characterization and mechanical properties of carbonated-hydroxyapatite prepared by mechanochemical synthesis. Mater Chem Phys 190:209–218
18. Zawrah MF, Essawy RA, Zayed HA, Abdel-Fattah AH, Taha MA (2014) Mechanical alloying, sintering and characterization of Al_2O_3-20 wt.%-Cu nanocomposite. Ceram Int 40:31–38
19. Taha MA, Nassar AH, Zawrah MF (2017) Improvement of wetability, sinterability, mechanical and electrical properties of Al2O3-Ni nanocomposites prepared by mechanical alloying. Ceram Int 43(4):3576–3582
20. Kokubo T, Takadama H (2006) How useful is SBF in pre predicting in vivo bone bioactivity. Biomater 27(15):2907–2915
21. Kokubo T, Kushitani H, Sakka S, Kitsugi T, Yamamuro T (1990) Solutions able to reproduce in vivo surface-structure changes in bioactive glass-ceramics A-W. J Biomed Mater Res A 24:721–734
22. Siqueira RL, Zanotto E (2013) The influence of phosphorus precursors on the synthesis and bioactivity of $SiO_2\text{-}CaO\text{-}P_2O_5$ sol-gel glasses and glass-ceramics. Mater Sci Mater Med 24:365–79

23. Kaur M, Mahajan M, Bhatia M, Kaur S, Singh L (2014) Preparation and characterization of rare earth doped phosphate glasses. i-Manager's J Mater Sci. **2**(1)
24. Massera J, Breillot MV, Törngren B, Glorieux B, Hupa L (2014) Effect of CeO_2 doping on thermal, optical, structural and in vitro properties of a phosphate based bioactive glass. Non-Cryst Solids 402:28–35
25. Aina V, Perardi A, Bergandi L, Malavasi G, Menabue L, Morterra C, Ghigo D (2007) Cytotoxicity of zinc-containing bioactive glasses in contact with human osteoblasts. Chem-Biol Interact 167:207–18
26. Srivastava AK, Pyare R (2012) Characterization of ZnO substituted 45S5 bioactive glasses and glass-ceramics. J Mater Sci Res 1(2):207–20
27. Sych O, Gunduz O, Pinchuk N, Stan GE, Oktar FN (2016) Tissue engineering scaffolds from La_2O_3-hydroxyapatite/boron glass composites. J Aust Ceram Soc 52(2):103–10
28. Wers E, Bunetel L, Oudadesse H, Lefeuvre B, Girot LA, Mostafa A, Pellen P (2013) Effect of copper and zinc on the bioactivity and cells viability of bioactive glasses. Bioceram Dev Appl 1:1–3
29. Kokubo T, Kushitani H, Ohtsuki C, Sakka S (1992) Chemical reaction of bioactive glass and glass-ceramics with a simulated body fluid. Mater Sci Mater Med 3:79–83
30. Stanciu GA, Sandulescu I, Savu B, Stanciu SG, Paraskevopoulos KM, Chatzistavrou X, Kontonasaki E, Koidis P (2007) Investigation of the hydroxyapatite growth on bioactive glass surface. Biomed Pharm Eng 1:34–9
31. Tohamy KM, Soliman IE, Motawea AE, Aboelnasr MA (2015) Synthesis, characterization and bioactive study of borosilicate sol-gel glass. Nat Sci 13(8):145–54
32. Abo-Naf SM, Khalil EM, El-Sayed EM, Zayed HA, Youness RA (2015) In vitro bioactivity evaluation, mechanical properties and microstructural characterization of Na_2O-CaO-B_2O_3-P_2O_5 glasses. Spectrochim Acta A 144:88–98
33. Fu H, Fu Q, Zhou N, Huang W, Rahaman MN (2009) In vitro evaluation of borate-based bioactive glass scaffolds prepared by a polymer foam replication method. Mater Sci Eng C29:2275–81
34. Salman SM, Salama SN, Abo-Mosallam H (2015) The crystallization behavior and bioactivity of wollastonite glass-ceramic based on Na_2O-K_2O-CaO-SiO_2-F glass system. Asian Ceram Soc 3:255–61.26
35. Pickup DM, Valappil SP, Moss RM, Twyman HL, Guerry P, Smith ME, Wilson M, Knowles JC, Newport RJ (2009) Preparation, structural characterization and antibacterial properties of Ga-doped sol-gel phosphate-based glass. J Mater Sci 44:1858–67
36. Valappil SP, Ready D, Abou Neel EA, Pickup DM, Chrzanowski W, O'Dell LA, Newport RJ, Smith ME, Wilson M, Knowles JC (2008) Antimicrobial gallium-doped phosphate-based glasses. Adv Funct Mater 18:732–41
37. Barralet J, Best S, Bonfield W (1998) Carbonate substitution in precipitated hydroxyapatite: An investigation into the effects of reaction temperature and bicarbonate ion concentration. J Biomed Mater Res 41:79–86
38. Huang W, Rahaman MN, Day DE, Li Y (2006) Mechanisms for converting bioactive silicate, borate and borosilicate glasses to hydroxyapatite in dilute phosphate solutions. Phys Chem Glass Eur J Glass Sci Tech B 47(6):1–12
39. Li Y, Coughlan A, Laffir FR, Pradhan D, Mellott NP, Wren AW (2013) Investigating the mechanical durability of bioactive glasses as a function of structure, solubility and inCubation time. Non-Cryst Solids 380:25–34
40. Li P, Kangasniemi I, De Groot K, Kokubo T (1994) Bone-like hydroxyapatite induction by a gel-derived titania on a titanium substrate. Am Ceram Soc 5:1307–12
41. Ho W, Lai C, Hsu H, Wu S (2010) Surface modification of a Ti-7.5 Mo alloy using NaOH treatment and Bioglass® coating. Mater Sci Mater Med 21:1479–88
42. Elwan RL, Al-Shathly MR (2014) Microstructural characterization and in vitro bioactivity of SrO-SiO_2-Na_2O-CaO-B_2O_3-P_2O_5 glasses. Life Sci J 11(12s):36–46
43. Singh KS, Srinivasan A (2010) Bioactivity of SiO_2-CaO-P_2O_5-Na_2O glasses containing zinc-iron oxide. Appl Surf Sci 256:1725–30
44. Leonelli C, Lusvardi G, Malavasi G, Menabue L, Tonelli M (2003) Synthesis and characterization of cerium-doped glasses and in vitro evaluation of bioactivity. Non-Cry Solids 316(2-3):198–216
45. Bellucci D, Cannillo V, Sola A, Chiellini F, Gazzarri M, Migone C (2011) Macroporous Bioglass®-derived scaffolds for bone tissue regeneration. Ceram Int 37:1575–85
46. Cabal B, Alou L, Couceiro R, Cafini F, Couceiro R, Tejeda LE, Guitian F, Torrecillas R, Maya JS (2014) A new biocompatible and antibacterial free glass-ceramic for medical applications. Sci Rep 5440(4):1–9
47. Deliormanh AM (2016) Electrospun cerium and gallium-containing silicate based 13-93 bioactive glass fibers for biomedical applications. Ceram Int 42(1):897–906
48. Pourshahrestani S, Zeimaran E, Kadri NA, Gargiulo N, Samuel S, Naveen SV, Kamarul T, Towler MR (2016) Gallium-containing mesoporous bioactive glass with potent hemostatic activity and antibacterial efficacy. Mater Chem B 4:71–86
49. Shelke VA, Jadhav SM, Shankarwar SG, Munde AS, Chondhekar TK (2011) Synthesis, characterization, antibacterial and antifungal studies of some transition and rare earth metal complexes of N-Benzylidene-2-Hydroxybenzohydrazine. Bull Chem Soc Ethiop 25(3):381–91
50. Jing FJ, Huang N, Liu YW, Zhang W, Zhao XB, Fu RKY, Shao ZY, Chen JY, Leng YX, Liu XY, Chu PK (2008) Hemocompatibility and antibacterial properties of lanthanum oxide films synthesized by dual plasma deposition. J Biomed Mater Res A 87(4):1027–33